Self-Affine Surface Morphology of Plastically Deformed Metals

Michael Zaiser,[1] Frederic Madani Grasset,[1,2] Vasileios Koutsos,[1] and Elias C. Aifantis[2]

[1]*Centre for Materials Science and Engineering, The University of Edinburgh, The King's Buildings, Sanderson Building, Edinburgh EH9 3JL, United Kingdom*

[2]*Laboratory of Mechanics of Materials, Aristotle University of Thessaloniki, 54006 Thessaloniki, Greece*

(Received 3 May 2004; published 5 November 2004)

We analyze the surface morphology of metals after plastic deformation over a range of scales from 10 nm to 2 mm using atomic force microscopy and scanning white-light interferometry. We demonstrate that an initially smooth surface during deformation develops self-affine roughness over almost 4 orders of magnitude in scale. The Hurst exponent H of one-dimensional surface profiles initially decreases with increasing strain and then stabilizes at $H \approx 0.75$. We show that the profiles can be mathematically modeled as graphs of a fractional Brownian motion. Our findings can be understood in terms of a fractal distribution of plastic strain within the deformed samples.

DOI: 10.1103/PhysRevLett.93.195507 PACS numbers: 62.20.Fe, 68.35.–p, 89.75.–k

According to the traditional paradigm implicit in continuum models of plasticity, plastic deformation under homogeneous loads and in the absence of so-called plastic instabilities is expected to proceed in a smooth and spatially homogeneous manner. Fluctuations, if any, are supposed to average out above the scale of a "representative volume element" that is assumed to be small in comparison with macroscopic dimensions (or, indeed, in comparison with the scale of any problem to which continuum modeling is applied). Recently for crystals deforming by dislocation glide, this paradigm has been challenged theoretically and experimentally [1–6]. Weiss *et al.* demonstrated that plastic flow of single-glide oriented ice single crystals proceeds in a temporally intermittent manner characterized by a sequence of large "deformation bursts" [1,3]. By monitoring acoustic emission, it was demonstrated that the burst sizes (characterized by the acoustic energy released during a burst) obey a scale-free power-law distribution over more than 6 orders of magnitude in energy [1]. Dislocation dynamics simulations showed qualitatively similar behavior [1,2]. These findings were interpreted as dynamical critical phenomena in a slowly driven nonequilibrium system [4,5] where the dislocation ensemble in a plastically deforming crystal is close to a critical point ("yielding transition" [4]).

Temporal intermittency of plastic flow goes along with spatial heterogeneity. This has been long known to metallurgists who observed pronounced surface traces ("slip lines") resulting from the collective motion of many dislocations. By monitoring the evolution of surface features it is therefore possible to study collective behavior in plastic flow. However, most investigations (for an overview, see [7]) have focused on the evolution of single slip lines or slip line bundles, i.e., the motion of isolated dislocation groups. Long-range correlations within the slip pattern have only occasionally been studied. Konstantinidis and Aifantis [8] used a wavelet transform to investigate the slip pattern of a Fe_3Al single crystal on multiple scales between 0.1 and 50 μm but did not quantitatively analyze their data in view of scale-invariant behavior. Kleiser and Bocek [9] report a self-similar pattern of slip lines in Cu single crystals on scales between 0.06 and 2 μm and determine a fractal dimension $D_F \approx 0.5$ for the set of intersection points between the slip lines and a line normal to the slip direction.

Recently, Weiss and Marsan [6] investigated the three-dimensional patterning of slip on macroscopic scales. By recording acoustic emission with multiple transducers and using spatial triangulation, they determined the 3D distribution of slip bursts in the volume of an ice single crystal. This investigation demonstrated that the slip burst pattern on macroscopic scales (0.6 mm to 10 mm) exhibits features of a fractal set with correlation dimension $D_C \approx 2.5$. However, due to the limited spatial resolution of the technique, no information about the slip distribution on smaller scales could be obtained.

In the present study we pursue a slightly different approach for assessing spatial correlations in plastic deformation from the nanoscopic to the macroscopic scale. Instead of directly studying the distribution of plastic strain in the bulk or on the surface of the sample, we monitor the evolution of the surface profile. One-dimensional surface profiles evolving from an initially smooth surface can be directly related to the plastic distortion at the surface: if we use a local coordinate system such that the x direction corresponds to the direction of a one-dimensional surface profile and the y direction to the surface normal, then the derivative $y_x = \partial y/\partial x$ of the profile $y(x)$ equals the component β_{yx} of the plastic distortion tensor. Long-range correlations in the plastic strain pattern can be detected since they give rise to characteristic modifications of the surface morphology—specifically speaking, power-law correlations in the spatial distribution of plastic strain lead to the emergence of self-affine surface profiles with a Hurst exponent $H > 0.5$ (cf. below).

The statistical properties of a self-affine profile $y(x)$ are invariant under the scaling transformation $x \rightarrow \lambda x$, $y \rightarrow \lambda^H y$. The roughness exponent or Hurst exponent H can be related to a fractal dimension D_F ("box dimension") of the profile through $D_F = 2 - H$ [10]. Self-affine behavior is abundant in natural surfaces; most prominent examples in materials physics are fracture surfaces whose large-scale roughness can be characterized by a universal (material-independent) exponent $H \approx 0.8$ [11]. In the present Letter we report for the first time an analysis of the surface structure of plastically deformed metal samples in terms of self-affine properties. We applied a combination of atomic force microscopy (AFM) and scanning white-light interferometry (SWLI) to quantitatively characterize the surface morphology over a range of scales between 10 nm and 2 mm. AFM scans (512×512 pixels) were taken over areas of 26 μm $\times$ 26 μm and 6 μm $\times$ 6 μm using a PicoSPM (Molecular Imaging) in constant deflection mode with a medium range scanner and a cantilever (Mikromasch, Ultrasharp) with a nominal spring constant of 1.75 N/m and tip curvature radius 10 nm; the rms vertical noise amplitude was less than 0.05 nm. SWLI (New View 100, Zygo) scans were performed over areas of 130 μm $\times$ 2000 μm with a lateral resolution of 0.6 μm and a vertical resolution of 0.5 nm. From the scans, typically 4–5 surface profiles were taken in the direction of the specimen axis and 2–3 profiles normal to that direction.

Polycrystalline copper samples of 99.9% nominal purity and 40 μm average grain size were electropolished to obtain a surface with low small-scale roughness (average rms roughness 2.2 ± 0.4 nm as determined from five AFM profiles of 6 μm length). Residual surface waviness persisted, however, on scales above 100 μm. After characterizing the initial surface, the samples were deformed in tension on a standard tensile-testing machine (Instron series 3360). Testing was done at room temperature with an imposed strain rate $\dot{\epsilon} = 1.5 \times 10^{-3}$ s^{-1}. At the total (engineering) strains $\epsilon = 2.3\%$ (tensile stress $\sigma =$ 70 MPa), 5.5 % ($\sigma = 122$ MPa), 9.6 % ($\sigma = 160$ MPa), 17.8 % ($\sigma = 199$ MPa), and 23 % ($\sigma = 215$ MPa), the sample was unloaded and AFM and SWLI scans were taken in a similar manner as before deformation. The sequence of surface morphology investigations was ended at the onset of macroscopic deformation localization (necking).

Typical surface profiles are shown in Fig. 1 representing an AFM profile obtained from a 26 μm $\times$ 26 μm scan and a SWLI profile. To investigate a possible self-affine structure, mean height differences $\langle |y(x) - y(x + L)| \rangle$ were evaluated as a function of L for each of the AFM and SWLI profiles by averaging over all pairs $(x, x + L)$ within the profile. Self-affine behavior implies that

$$\langle |y(x) - y(x + L)| \rangle \propto L^H. \quad (1)$$

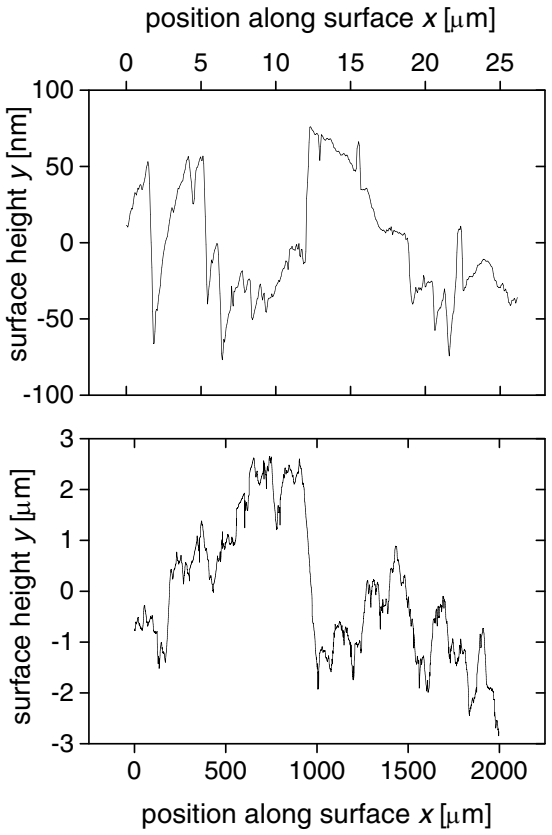

FIG. 1. Surface profiles taken at $\epsilon = 9.6\%$; top: AFM profile; bottom: SWLI profile; the x direction is parallel to the direction of the tensile axis; roughness plots corresponding to these profiles are shown in Fig. 2.

Hence, double-logarithmic plots of $\langle |y(x) - y(x + L)| \rangle$ vs L should exhibit a linear scaling regime with slope H. Such "roughness plots" are shown in Fig. 2. Typical plots exhibit linear scaling regimes extending between 0.05 and 5 μm for the AFM and between 0.5 and 100 μm for the SWLI profiles. Hurst exponents deduced from the slope of the scaling regimes are similar for AFM and SWLI profiles, and also the absolute values of $\langle |y(x) - y(x + L)| \rangle$ are similar across the region of overlap of the roughness plots. Hence, we observe continuous scaling over almost 4 orders of magnitude. Surface profiles $y(z)$ taken in the direction normal to the tensile axis exhibit scaling with similar exponents, although the length of the self-affine scaling regimes is reduced. Hurst exponents H determined from the roughness plots (and the corresponding fractal dimensions $D_F = 2 - H$) are compiled in Fig. 3. The error bars reflect the scatter of exponents obtained from different profiles taken at the same strain. It can be seen that the exponents initially decrease with increasing strain and then stabilize above $\epsilon \approx 10\%$ at a value of $H \approx 0.75$. It is important to note that the initial value of $H \approx 1$ does not reflect any surface roughness but simply stems from large-scale gradients on an almost smooth surface. Because of the waviness above 100 μm, shorter sections of the surface are generally

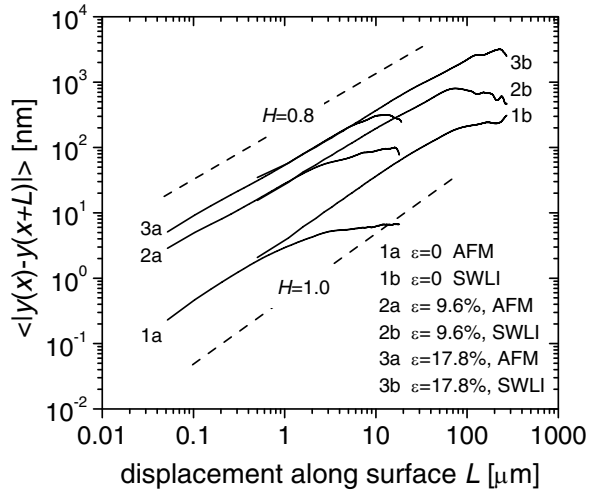

FIG. 2. Roughness plots (mean height difference vs distance along profile) for AFM and SWLI profiles obtained from the as-polished surface and after deformation to strains of 9.6% and 17.8%; the profiles for $\epsilon = 9.6\%$ are shown in Fig. 1.

inclined, which means that height differences grow linearly with distance. The Hurst exponent is therefore close to unity and also the fractal dimension of the one-dimensional profiles is $D_F \approx 1$, as it should be. On roughness plots obtained from the "short" AFM profiles taken from 6 μm $\times$ 6 μm scans, one observes on scales below 50–100 nm a crossover to a strain-independent Hurst exponent $H \approx 1$ since, on very small scales, one essentially "sees" the smooth—but inclined—initial surface in between the deformation-induced surface steps.

To further investigate the statistical surface properties in the different scale regimes, probability distributions $p(\Delta y_L)$ of surface height differences $\Delta y_L = y(x) - y(x + L)$ have been determined for profiles taken at $\epsilon = 9.6\%$. $L_0 = 0.5$ μm was taken as a reference, and height differences were normalized by the variance $y_0 = \langle \Delta y_{L_0}^2 \rangle^{0.5} = 27.08$ nm of the corresponding height difference distribution. Within the scaling regime $\xi_0 < L < \xi_1$ ($\xi_0 \approx 50$ nm, $\xi_1 \approx 100$ μm), probability distributions for different L can be collapsed by rescaling $\Delta y_L/y_0 \rightarrow (L/L_0)^H \Delta y_L/y_0$ with $H = 0.72$ (Fig. 4):

$$p([L/L_0]^H \Delta y_L/y_0) = p(\Delta y_{L_0}/y_0). \quad (2)$$

To assess the shape of the probability distributions, cumulative distributions normalized to unit variance have been represented on a probability scale (i.e., the error function appears as a straight line). The insert of Fig. 4 shows the distribution for $L = 2$ μm (full line) as well as two distributions for L outwith the scaling regime, namely, for $L = 40$ nm (dashed line) and $L = 160$ μm (dotted line). Distributions throughout the self-affine scaling regime are well approximated by Gaussian statistics, but the tails of distributions outwith the scaling regime exhibit characteristic deviations from Gaussian behavior. On scales below ξ_0 the surface exhibits flat regions separated by huge slip steps marking slip events. This leads to a leptokurtic distribution with heavy tails. On scales above ξ_1, on the other hand, the surface flattens and large height fluctuations are suppressed since the macroscopic slope of the SWLI profiles is by definition set to zero. This gives rise to platykurtic distributions with truncated tails.

The fact that the statistics is Gaussian throughout the scaling regime implies that the surface profiles $y(x)$ can be mathematically interpreted as graphs of fractional Brownian motions. This implies that the increments y_x exhibit long-range correlations given by [12]

$$\langle y_x(x) y_x(x') \rangle \propto |x - x'|^{2H-2}. \quad (3)$$

Since y_x equals the component β_{yx} of the plastic distortion tensor at the surface, our observations yield evidence for power-law correlations in the distribution of plastic strain. From the correlation integral

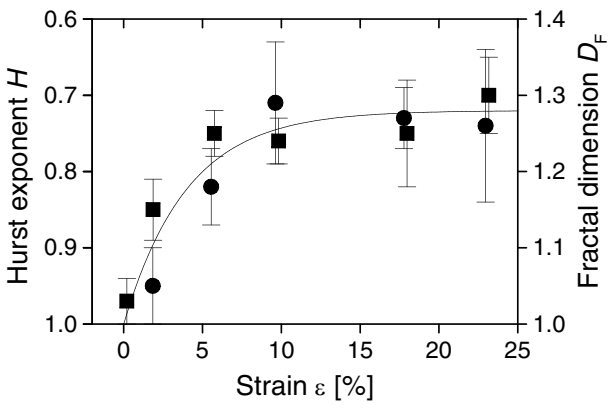

FIG. 3. Fractal dimension and Hurst exponent as a function of strain, squares: values determined from SWLI profiles, circles: values determined from AFM profiles; each value represents an average over five profiles; full line: guide to the eye.

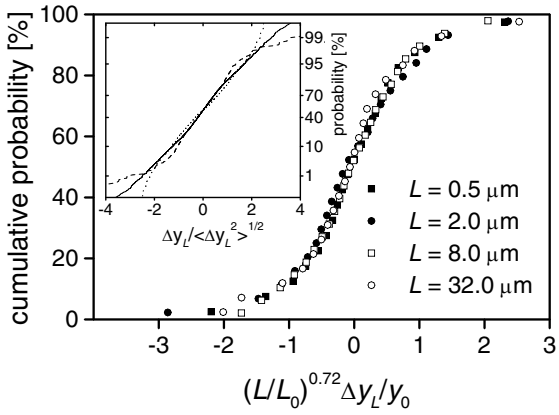

FIG. 4. Scaling collapse of height difference distributions obtained from AFM and SWLI profiles ($\epsilon = 9.6\%$); insert: distributions normalized to unit variance for $L = 40$ nm (dashed line), $L = 5$ μm (full line), and $L = 160$ μm (dotted line).

$$I(R) = \int_{|x-x'|<R} \langle y_x(x) y_x(x') \rangle d(x - x') \propto R^{2H-1} \quad (4)$$

we deduce a correlation dimension $D_C = 2H - 1 \approx 0.5$ for the one-dimensional strain pattern underlying the surface profile. The value $D_C \approx 0.5$ is consistent with the fractal dimension of slip line patterns reported by Kleiser and Bocek [9]. A dimension of 0.5 for a one-dimensional strain pattern is also consistent with the dimension $D_F = 2.5$ for the three-dimensional pattern of slip events measured by Weiss and Marsan [6]. These investigations were performed on single crystals; due to experimental limitations the scaling regimes cover only about 1 order of magnitude. Our results demonstrate that the strain pattern in polycrystals exhibits an analogous self-similar behavior, which by combining different experimental techniques can be traced over almost 4 orders of magnitude in scale.

More investigations are required to decide whether the Hurst exponent $H \approx 0.75$ that we determine for deformed metal surfaces is universal, i.e., independent of material and deformation conditions. Further investigations are also needed to establish the nature of the boundaries of the self-affine scaling regime. The lower bound of the scaling regime can be related to the spacing between individual "slip events" between which the surface remains unchanged by the deformation. The upper boundary ξ_1 of the scaling regime, which defines the correlation length of the self-affine surface pattern, is of the same order of magnitude as the grain size (40 μm), and one may reasonably conjecture that the range of correlations in the dislocation dynamics, and therefore in the slip pattern, is limited by the grain size. However, ξ_1 also roughly matches the "wavelength" of about 100 μm, which stems from the initial surface waviness and might therefore simply be an artefact of the initial conditions. Further experiments, preferentially using both mechanical and electropolishing for surface preparation, and including single crystals, are needed to clarify this issue.

In view of plasticity models using coarse-grained strain variables, our results indicate that strain fluctuations may average out rather slowly on scales below the correlation length. The strain fluctuation on scale L can be estimated as $\Delta\epsilon_L \sim \Delta y_L/L$. At the lower end of the self-affine scaling regime ($\xi_0 \approx 50$ nm), fluctuations are of the same order of magnitude as the average strain. Within the scaling regime, strain fluctuations decrease like $(\xi_0/L)^{1-H}$ if averaged over the length L; for $(1 - H) \approx 0.25$ we find that the residual strain fluctuations at the upper end of the scaling regime ($\xi_1 \approx 100$ μm) are still about 15% of the average strain. This observation explains why it is possible to detect significant strain fluctuations even on macroscopic scales [13,14].

The fact that the Hurst exponent of deformed metal surfaces is quite similar to that of fracture surfaces raises the fundamental question whether there is a universal mechanism underlying both observations, or whether the similarity of exponents is incidental. Crystal plasticity is a bulk phenomenon that only indirectly affects the surface, whereas fracture is directly governed by surface and interface properties. However, this does not preclude the possibility of a common theoretical treatment within the framework of nonequilibrium critical phenomena. Finally, an intriguing question concerns the relationship between deformation-induced surface morphology and defect microstructure. Fractal dislocation cell patterns have been reported in Cu single crystals deformed uniaxially in near-cube orientations [15]. Hughes and coworkers, on the other hand, have performed microstructure investigations for a wide range of materials and deformation conditions including Cu polycrystals (see [16] and references therein) and conclude that dislocation patterns in deformed metals can be characterized in terms of universal cell size and orientation distributions that are *not* compatible with scale-free behavior as there is a well-defined characteristic cell size. This discrepancy indicates that there is no one-to-one correspondence between defect microstructure and plastic flow patterns and that different mechanisms may govern the spatial organization of slip, and the patterning of deformation-induced defects.

We acknowledge financial support by the European Commission under RTN/DEFINO HPRN-CT 2002-00198 and by EPSRC under Grants No. GR/S20406/01 and No. GR/R43181/01.

[1] M.-C. Miguel *et al.*, Nature (London) **410**, 667 (2001).
[2] M.-C. Miguel *et al.*, Mater. Sci. Eng. A **309-310**, 324 (2001).
[3] J. Weiss *et al.*, Mater. Sci. Eng. A **309-310**, 360 (2001).
[4] M. Zaiser, Mater. Sci. Eng. A **309-310**, 304 (2001).
[5] M.-C. Miguel, A. Vespignani, M. Zaiser, and S. Zapperi, Phys. Rev. Lett. **89**, 165501 (2002).
[6] J. Weiss and D. Marsan, Science **299**, 89 (2003).
[7] H. Neuhauser, *Dislocations in Solids*, edited by F. R. N. Nabarro (North Holland, Amsterdam, 1983), p. 319.
[8] A. A. Konstantinidis and E. C. Aifantis, J. Eng. Mater. Technol. **124**, 358 (2002).
[9] T. Kleiser and M. Bocek, Z. Metallkd. **77**, 582 (1986).
[10] B. Mandelbrot, Phys. Scr. **32**, 257 (1985).
[11] E. Bouchaud, J. Phys. Condens. Matter **9**, 4319 (1997).
[12] N. Enriquez, Stochastic Processes and Their Applications **109**, 203 (2004).
[13] J. Diehl, Z. Metallkd. **47**, 331 (1956); **47**, 411 (1956).
[14] M. Zaiser and P. Hähner, Philos. Mag. Lett. **73**, 369 (1996).
[15] P. Hähner, K. Bay, and M. Zaiser, Phys. Rev. Lett. **81**, 2470 (1998).
[16] A. Godfrey and D. A. Hughes, Scr. Mater. **51**, 831 (2004).